Study of recycling blast furnace dust by magnetization roasting with straw charcoal as reductant

Jinrong Ju [1,2,3], Yali Feng [1], Haoran Li [2,3], Qian Zhang [1]

[1] Civil and Resource Engineering School, University of Science and Technology Beijing, Beijing 100083, China

[2] Key Laboratory of Biochemical Engineering, Institute of Process Engineering, Chinese Academy of Sciences, Beijing 100190, China

[3] University of Chinese Academy of Sciences, Beijing 100049, China

Corresponding authors: ylfeng126@126.com (Yali Feng), hrli@ipe.ac.cn (Haoran. Li).

Abstract: Blast furnace dust generated in the iron-making process not only contains a large amount of iron but also the widely used non-ferrous metal zinc, which is classified as hazardous waste. In this study, the process of recycling blast furnace dust by magnetization roasting with straw charcoal as the reductant is proposed, and the mechanism of magnetization roasting was explored through thermodynamic analysis, X-ray diffraction analysis, and thermogravimetric analysis. The results for the thermodynamic analysis showed that the reduction of blast furnace dust by the straw charcoal was feasible theoretically. The increase in the roasting temperature not only promoted the reduction of hematite (Fe_2O_3) but also reduced zinc ferrite ($ZnFe_2O_4$) to Fe_3O_4 and ZnO. The results showed that almost all Fe_2O_3 and $ZnFe_2O_4$ in the blast furnace dust were reduced to Fe_3O_4 and ZnO under the conditions of straw charcoal amount of 6%, the roasting temperature of 750 ℃, and the roasting time of 60 min. Then, the iron concentrate with the iron recovery of 85.61% and an iron grade of 63.50% was obtained by the magnetic separation. Meanwhile, the grade of zinc in the iron concentrate was 0.19%. Finally, the flowsheet of simultaneously recovering iron and zinc from the blast furnace dust was put forward, which could realize that 85.61% of iron was recovered and 92.57% of zinc was extracted into the solution.

Keywords: blast furnace dust, straw charcoal, magnetization roasting, hematite, zinc ferrite

1. Introduction

Blast furnace dust is a hazardous waste produced in the iron-making process (Zhang et al., 2017). A gravity dust collector, cyclone dust collector, bag dust collector, and other devices were used to obtain blast furnace dust (Luo et al., 2022). It contains zinc, iron, carbon, and other ferrous metals and nonferrous metals, and is classified as typical secondary zinc and iron resources (Leclerc et al., 2002; Li et al., 2015; Lanzerstorfer, 2017). The particle size of blast furnace dust is generally between 40-120 μm, with good fluidity (Nayak, 2022). Therefore, it is easy to cause secondary pollution, especially when the dust particles are less than 5 μm, which can be suspended in the air for a long time.

According to statistics, the global crude steel output in 2019 was about 1.87 billion tons, an increase of 3.4% over 2018 (Ye et al., 2021). With the rapid development of the social economy, the demand for iron and steel is increasing, the blast furnace tends to become larger, and the output of blast furnace dust increases with the years. To recover iron resources, the blast furnace dust as sintering material directly back to the blast furnace iron-making process. However, the accumulation of volatile metals such as zinc and lead will reduce the utilization coefficient and service life of blast furnaces (Mansfeldt and Dohrmann, 2004; Yang et al., 2009). Moreover, simple landfilling or piling treatment is not economical because of the environmental impact and waste of precious metal resources in blast furnace dust (Mansfeldt and Dohrmann, 2004).

In order to extract and utilize valuable metal elements from the blast furnace dust, several different treatment methods have been proposed, including pyrometallurgical and hydrometallurgical

methods (Xu et al., 2020). Among pyrometallurgical methods, sintering (Makkonen et al., 2002; Chun and Zhu, 2015; Lanzerstorfer et al., 2015) and rotary hearth furnace (Hu et al., 2016; Wu et al., 2018) are the most widely used. This is because of the high iron and carbon content of blast furnace dust, which is a good recycling material to replace raw materials and solid fuels in the sintering process (Shen et al., 2010). Although the metal recovery of the pyrometallurgical recovery process is high, due to the fine particle size of dust and high moisture content, resulting in poor air permeability and poor sintering effect (Lin et al., 2017; Zhong et al., 2018). Consequently, the sintering method for the recovery of blast furnace ash has certain limitations. Based on the characteristics that zinc oxide can be reduced to metallic vapor by reducing gas, a rotary kiln flue gas volatilization technology was proposed to recover zinc from low grade zinc blast furnace dust (Hu et al., 2014; Hu et al., 2017; Wu et al., 2017). However, only zinc is recovered in this way while other valuable elements such as iron and carbon become pollutants so that the output of secondary waste after flue gas volatilization is almost equal to the amount of initial blast furnace dust (Hu et al., 2018). Although the above traditional pyrometallurgical process has high metal recovery efficiency, it has disadvantages such as low productivity, serious environmental pollution, and large energy consumption (Lin et al., 2017; Ye et al., 2021). Moreover, the extensive use of anthracite reductants has posed a great threat to the ecological environment. The hydrometallurgical method is mainly to extract zinc from blast furnace dust by using various leaching agents (Asadi Zeydabadi et al., 1997; Das et al., 2007; Steer and Griffiths, 2013; Zhang et al., 2017). Nevertheless, due to relatively high production costs, they are only suitable for processing blast furnace dust with high zinc content (Halli et al., 2017; Zhang et al., 2019). Moreover, the amount of leaching agent is large, and the treatment of waste liquid is difficult. Therefore, the development of an effective treatment process for blast furnace dust is of great significance to resource recovery and environmental protection.

Crop straw is a common agricultural by-product (Guo et al., 2021). In China, a large number of straws are directly burned in the open air, resulting in a large number of harmful gases that pollute the atmosphere and have been banned in China in recent years (Kanabkaew and Nguyen, 2011; Liu et al., 2019). Meanwhile, straw, as a kind of biomass, is considered to be a kind of renewable clean, and safe energy, which is conducive to protecting the environment, energy security, and economy (Hajinajaf et al., 2021). Straw is increasingly being used for sustainable energy, including the production of straw charcoal through carbonization (Seglah et al., 2020). It is concluded that straw charcoal can be used as a substitute reducing agent for traditional coal in the future reduction system.

In this study, the process of recycling blast furnace dust by the magnetization roasting using straw charcoal as a reductant was proposed. The effects of straw charcoal dosage, roasting time, and roasting temperature on the reduction effect were systematically investigated by a single factor conditional experiment. At the same time, thermodynamic analysis, thermogravimetric analysis (TG), derivative thermogravimetry (DTG), and X-ray diffraction (XRD) analyses were used to study the chemical reaction behavior and phase structure change of iron and zinc during the magnetization roasting process. Moreover, the flowsheet for simultaneous recovery of iron and zinc from blast furnace dust was presented.

2.   Materials and methods

2.1. Raw Materials

The blast furnace dust used in this study was provided by an iron and steel company in Liaoning Province, China. The industrial analysis and main chemical composition of blast furnace dust were analyzed by industrial analyzer and X-ray fluorescence spectrometry. The results for industrial analysis and the chemical composition for of blast furnace dust are presented in Tables 1 and 2, respectively. It can be seen from Table 1 that the content of fixed carbon and ash in blast furnace dust is 11.32% and 77.05%, respectively. According to the analysis of the chemical compositions (Table 2), the content of Fe and ZnO in blast furnace dust is 41.98% and 5.67%, among which the main impurities are SiO_2, CaO, and Al_2O_3 at 15.47%, 9.63%, and 4.69%, respectively. The XRD pattern of blast furnace dust shown in Fig. 1 indicates that the hematite (Fe_2O_3), quartz (SiO_2), and zinc ferrite ($ZnFe_2O_4$) are the main components, while calcio-olivine (Ca_2SiO_4) and calcium oxide (CaO) are the minor components.

The straw charcoal was provided by a company in Beijing. The industrial analysis of straw charcoal was analyzed by industrial analyzer and ash compositions was analyzed by X-ray fluorescence spectrometry. The industrial analysis and ash compositions results of the straw charcoal are shown in Table 3, in which the fixed carbon, ash, volatiles, and moisture content in the straw charcoal are 80.17%, 3.97%, 6.12%, and 9.74%, respectively. Ash mainly consists of oxides of silicon, calcium, magnesium, aluminum, iron, and sodium.

Table 1. Industrial analysis of the blast furnace dust

Component	Fixed carbon	Ash	Volatiles	Moisture
Content (wt.%)	11.32	77.05	10.37	1.26

Table 2. Main chemical components of the blast furnace dust

Component	TFe*	SiO_2	CaO	Al_2O_3	ZnO	MgO	Na_2O	S	P
Content (wt.%)	41.98	15.47	9.63	4.69	5.67	1.61	1.25	1.43	0.03

* TFe is the content of all iron elements in the blast furnace dust
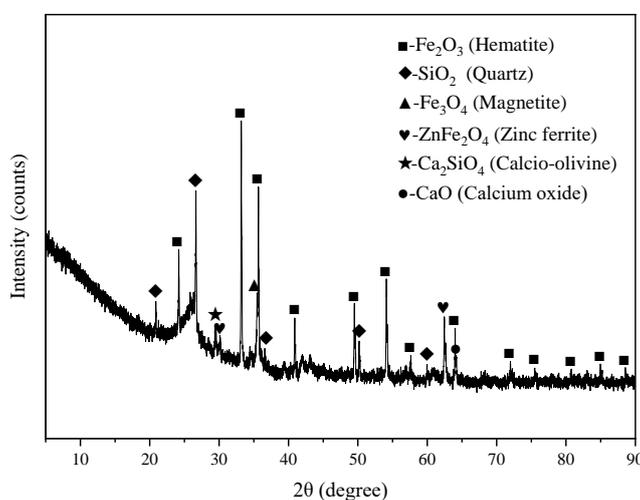
Fig. 1 X-ray diffraction (XRD) patterns of the blast furnace dust

Table 3. Industrial analysis and ash compositions of the straw charcoal

Component	Fixed carbon	Ash	Volatiles	Moisture	Ash					
					SiO_2	CaO	MgO	Al_2O_3	Fe_2O_3	Na_2O
Content (wt.%)	80.17	3.97	6.12	9.74	1.25	0.51	0.43	0.57	0.28	0.23

2.2. Methods

Fig. 2 shows the schematic diagram of the magnetization roasting experimental set-up. In this study, the straw charcoal was used as the reductant to roast with blast furnace dust in an oxygen-free environment. Hematite (Fe_2O_3) in the blast furnace dust was reduced to magnetite (Fe_3O_4) by the straw charcoal, hence iron was recycled by a magnetic separation. In the magnetization roasting experiment, the mass of blast furnace dust was 50 g. The amount of straw charcoal was based on the mass of blast furnace dust. The detailed experimental procedure is as follows: Firstly, the blast furnace dust was ground to less than 0.074 mm by the Laboratory CGQM conical ball mill and mixed evenly with straw charcoal according to a certain mass ratio (The mass of straw charcoal accounts for 0%-10% of that of blast furnace dust), and the well-mixed samples as required were put into a porcelain boat. The porcelain boat was put into a tube furnace. Then, N_2 was introduced into the tube furnace to remove the oxidizing atmosphere. In the whole experiment, the temperature in the tube furnace was increased to a predetermined temperature (600 ℃-800 ℃) at a heating rate of 20°min⁻¹, and

maintained at this temperature for a period of time (40 min-80 min); After the roasting process, the roasted products were taken out after the temperature cooling to room temperature. Finally, the roasted slag was ground and screened to obtain the samples with a particle size less than 0.074 mm for the magnetic separation experiment. The magnetic separation experiment was performed to recover iron from the roasted samples in a Davies magnetic separator (XCGS-50) at the magnetic intensity of 120 kA/m.

In each magnetic separation experiment, the 10 g of the roasted samples were placed in a 1000 cm³ beaker, about 500 cm³ of deionized water was added, and the mixtures were stirred for 5 min to fully wet the particle surface. First, the hose outlet at the lower end of the magnetic separation tube was closed, and the clean water was poured into the glass tube to be higher than the two magnetic poles, and then the magnetic separator was started. Then, the slurry was slowly poured into the glass tube, and the hose outlet at the lower end of the magnetic separation tube was opened, During the whole magnetic separation process, the liquid level in the glass tube was kept higher than the two magnetic poles. After the magnetic separation, rinsed the concentrate with clean water for 2 min, turned off the power supply, and flushed out the concentrate with clean water. Finally, concentrate and tailings were obtained by filtration and drying.

The leaching experiments were carried out in an electric heating magnetic stirrer. The 50 cm³ H_2SO_4 solution (0.5 mol/L) was taken to a 100 ml conical flask that was placed in an electric heating magnetic stirrer. Then, the 10 g tailings were added under the action of stirring. The slurry was heated to 40 °C for 90 min at a stirring speed of 500 rpm. After the reaction was finished, the leaching slurry was filtered to obtain the zinc-bearing filtrate and the leaching residues. The leaching efficiency of zinc was calculated according to the principle of mass conservation.

The 0.1 g of the roasted slag or magnetic concentrate was completely dissolved in mixed acid (20 cm³ HCl, 5 cm³ HNO_3, and 5 cm³ HF) and diluted to 100 cm³. The three acids were all purchased from Shanghai Maclean Biochemical Technology Co., LTD., and their purity was 37%, 68%, and 40%, respectively. The concentration of iron and zinc in the solution was determined by inductively coupled plasma emission spectrometry. According to the concentration of iron and zinc in the solution, the iron and zinc grade in the roasted slag and magnetic concentrate was determined. Based on the principle of conservation of mass, the iron recovery was calculated by Eq. (1).

$$\eta(\%) = \frac{m_1 \times \beta_1}{m_0 \times \beta_0} \times 100\% \tag{1}$$

where m_1 stands for the mass of iron concentrate, β_1 for the iron grade in iron concentrate, m_0 is the mass of roasted slag used in magnetic separation, and β_0 refers to the iron grade in roasted slag.
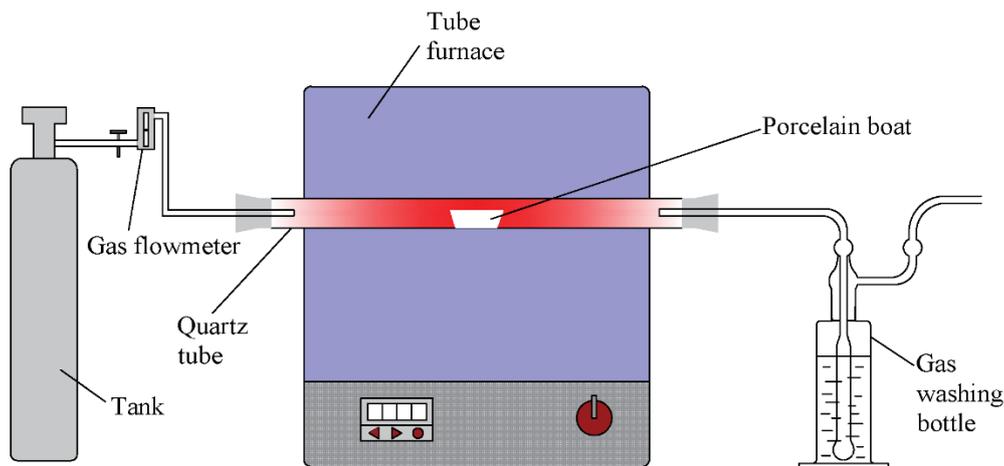
Fig. 2. Schematic diagram of the magnetization roasting experimental set-up

2.3. Characterization

X-ray fluorescence spectrometry (XRF: Axios, PANalytical B.V., Almelo, Netherlands) analysis for the sample was performed under the following conditions: non-attenuating 4 kW X-ray tube, 60 kW solid-

state generator power, and 160 mA current. X-ray diffractometry (XRD: Smartlab, Rigaku Corporation, Tokyo, Japan) was carried out at a scan range of 5° to 90° 2θ at a rate of 5° min⁻¹; The thermogravimetric analysis (METTLER TOLEDO, Switzerland) was performed under the protective gas at a 100 cm³/min flow rate. The concentration in the solution of iron and zinc was conducted by an inductively coupled plasma-atomic mission spectroscopy instrument (iCAP 6300, Thermo Scientific, America).

3.   Results and discussion

3.1. Effects of amount of straw charcoal on magnetization roasting and magnetic separation

Based on the results of thermodynamic analysis and preliminary exploration experiments, the influence of the amount of straw charcoal on the iron grade in magnetic concentrate, iron recovery, and zinc grade in magnetic concentrate was investigated under the conditions of magnetization roasting temperature of 700 ℃ and roasting time of 60 min, and the results are shown in Fig. 3.

Fig. 3a shows the iron grade and recovery under different amounts of straw charcoal; Fig. 3b is the zinc grade in magnetic concentrate under different amounts of straw charcoal. According to the industrial analysis results (Table 1) of blast furnace dust, the content of fixed carbon in blast furnace dust is 11.32%, which can also participate in the magnetization roasting process. Therefore, the magnetization roasting effect in the absence of straw charcoal was studied. It can be observed from Fig. 3a that the iron grade in magnetic concentrate obtained by magnetic separation was 54.27% and the iron recovery was 71.89% after magnetic roasting without adding reducing agents. However, the zinc grade in magnetic concentrate was as high as 1.74%, which indicated that the result of magnetization roasting was not ideal without adding reducing agents. When the amount of straw charcoal was increased from 2% to 6%, the iron grade and recovery increased continuously, while the grade of zinc in magnetic concentrate reduced. When the amount of straw charcoal was 6%, the iron grade and iron recovery were 62.07% and 83.76%, and the zinc grade in magnetic concentrate was decreased to 0.26%. When the amount of straw charcoal was increased to 8%, the iron grade remained unchanged and the iron recovery decreased. After that, when the amount of reducing agent was increased, the decreasing trend of iron grade and recovery was observed. Moreover, the increasing the amount of straw charcoal would increase the production cost. Therefore, it was finally determined that the best amount of straw charcoal was 6% of the blast furnace dust quality.
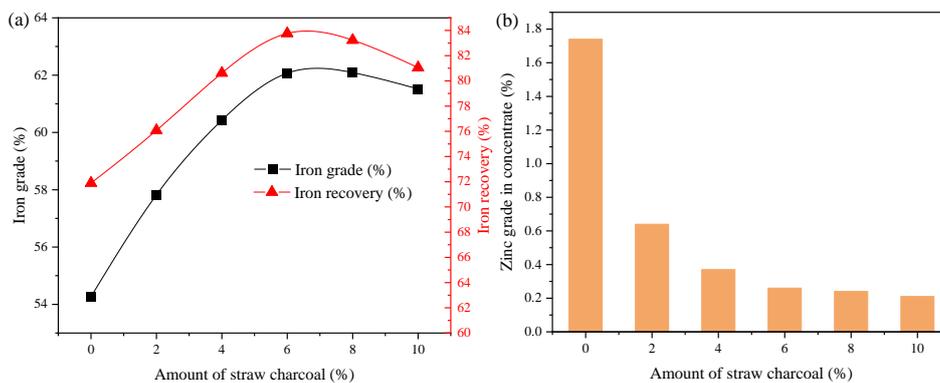
Fig. 3. Effect of amount of straw charcoal: (a) iron grade and recovery, (b) zinc grade in magnetic concentrate.

To explore the change of iron and zinc phases in the roasting slag at different amounts of reductants, the roasting slag with different amounts of straw charcoal was analyzed by XRD, and the results are shown in Fig. 4. As shown in Fig. 4, when no straw charcoal was added for the magnetization roasting, the main diffraction peak in the roasting slag had changed to Fe_3O_4. However, there were still many diffraction peaks of Fe_2O_3 and an obvious diffraction peak of $ZnFe_2O_4$ in the XRD patterns of the roasting slag. Therefore, the reductants were not enough to reduce Fe_2O_3 and $ZnFe_2O_4$ in blast furnace dust to Fe_3O_4 and ZnO, the iron grade in magnetic concentrate and recovery were low, and the zinc grade in magnetic concentrate was high. When the amount of straw charcoal was 2%, the diffraction peak of $ZnFe_2O_4$ disappeared and the diffraction peak of Fe_2O_3 weakened. When the amount of straw

charcoal was increased to 4%, ZnO was observed in the XRD pattern of roasting slag, but there was still a small amount of Fe_2O_3 diffraction peak. From the Fig. , it can be found that when the dosage of straw charcoal was 6%, the Fe_2O_3, and $ZnFe_2O_4$ in the blast furnace dust were basically all reduced to Fe_3O_4 and ZnO. The XRD peaks of the roasting slag with the 8% straw charcoal amount were consistent with the 6% straw carbon amount. Nevertheless, the diffraction peak of FeO was found in the XRD pattern of the roasting slag obtained when the amount of straw charcoal was 10%. It is due to the excessive reduction that part of Fe_3O_4 was reduced to FeO, so the magnetic separation effect became worse.
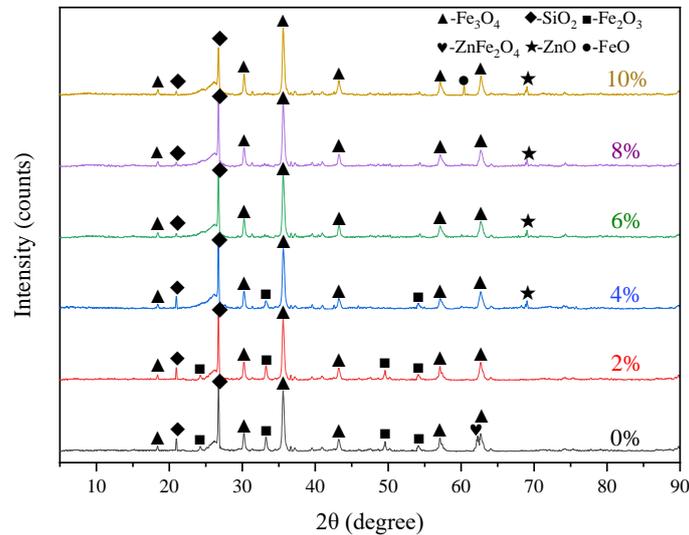
Fig. 4. XRD patterns of roasted slag with different amounts of straw charcoal

3.2. Effects of roasting temperature on magnetization roasting and magnetic separation

Based on the amount of reductant determined in Section 3.1, the effects of different magnetic roasting temperatures on iron grade in magnetic concentrate, iron recovery, and zinc grade in magnetic concentrate were studied under the conditions that the amount of straw charcoal was 6% and the magnetization roasting time was 60 min. The experimental results are shown in detail in Fig. 5.
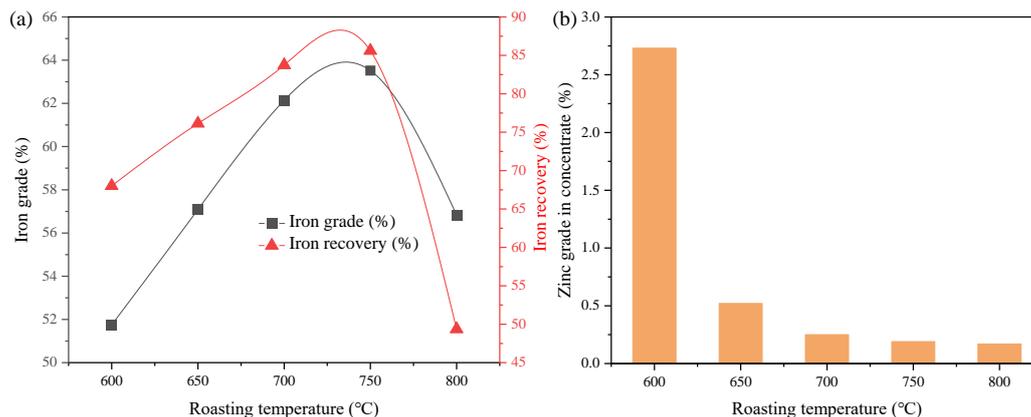
Fig. 5. Effect of roasting temperature: (a) iron grade and recovery, (b) zinc grade in magnetic concentrate.

Fig. 5a shows the iron grade and recovery under different roasting temperatures; Fig. 5b shows the zinc grade in magnetic concentrate under different roasting temperatures. It is obvious from Fig. 5a that the magnetization roasting temperature has a great influence on magnetic separation. When the magnetization roasting was carried out at 600 ℃, the iron grade in magnetic concentrate obtained by magnetic separation was only 51.75% and the iron recovery was 68.02%. At this temperature, the grade of zinc in magnetic concentrate was 2.73%, indicating that most of the zinc was retained in

magnetic concentrate, which may be caused by the incomplete decomposition of $ZnFe_2O_4$. As the increase of magnetization roasting temperature from 600 ℃ to 750 ℃, iron grade and recovery increased to 63.52% and 85.61% rapidly, and zinc grade in magnetic concentrate decreased to 0.19%. However, when the temperature of magnetization roasting increased to 800 ℃, the iron grade and recovery dropped sharply to 56.83% and 49.37%, which may be because part of Fe_3O_4 was over-reduced to FeO, so the magnetic separation effect was not ideal. After comprehensive consideration, 750 ℃ was determined as the optimal temperature for the magnetization roasting.

Fig. 6 shows the XRD patterns of the roasting slag obtained at different roasting temperatures. It can be seen from Fig. 7 that when the roasting temperature was 600 ℃, there were strong diffraction peaks of Fe_2O_3 and $ZnFe_2O_4$ in the XRD patterns of the roasting slag. With the roasting temperature rising to 650 ℃, the diffraction peak intensity of $ZnFe_2O_4$ decreased and that of Fe_3O_4 increased. However, at 650 ℃, there were still obvious Fe_2O_3 diffraction peaks in the slag, indicating that this temperature cannot meet the requirements of magnetization roasting. When the roasting temperature was 700 ℃ and 750 ℃, the phase composition of the roasting slag was the same, and the diffraction peaks of the XRD pattern were mainly Fe_3O_4, SiO_2, and ZnO. But, it can be observed that the diffraction peak intensity of ZnO in roasting slag was stronger than that at the roasting temperature of 700 ℃. When the roasting temperature rose to 800 ℃, not only did the strong diffraction peak of FeO appear in the roasting slag but also the diffraction peak of Fe_3O_4 weakened. The XRD patterns of the roasting slag obtained at different roasting temperatures perfectly explain the reason why iron grade in magnetic concentrate and recovery firstly increased and then decreased with the roasting temperature rising from 600 ℃ to 800 ℃.
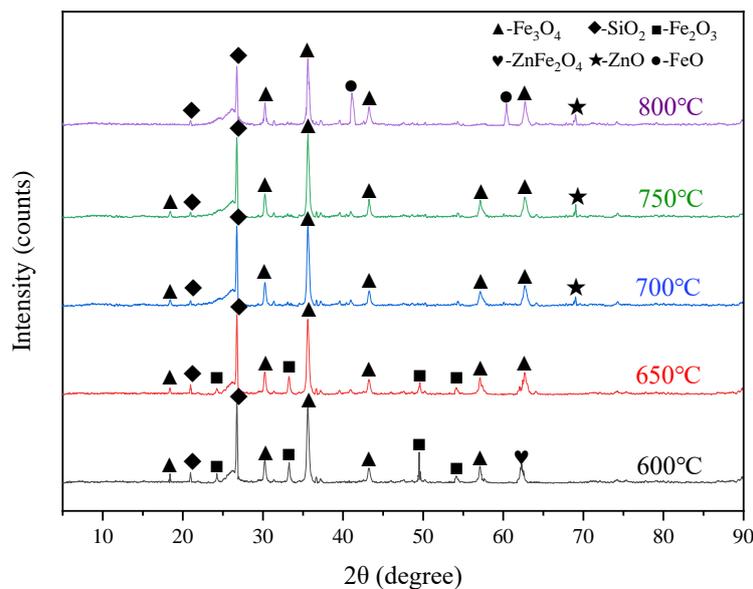
Fig. 6. XRD patterns of roasted slag with different roasting temperatures

3.3. Effects of roasting time on magnetization roasting and magnetic separation

Under the conditions of straw charcoal amount of 6% and magnetization roasting temperature of 700 ℃, the effect of the roasting time on the iron grade in magnetic concentrate, iron recovery, and zinc grade in magnetic concentrate was investigated, and the results are shown in Fig. 7.

Fig. 7a is the iron grade and recovery under different magnetization roasting times; Fig. 7b is the zinc grade in magnetic concentrate under different magnetization roasting times. As shown in Fig. 7, with the roasting time extending from 40 min to 80 min, iron grade and recovery increased firstly and then decreased, while zinc grade in magnetic concentrate decreased firstly and then remained stable. When the roasting time was 60 min, iron grade and iron recovery were 63.49% and 85.62%, respectively, and zinc grade in magnetic concentrate was 0.19%. After 60 min, the iron grade and iron recovery decreased gradually when the roasting time was extended. Therefore, the optimal roasting time was finally determined to be 60 min.
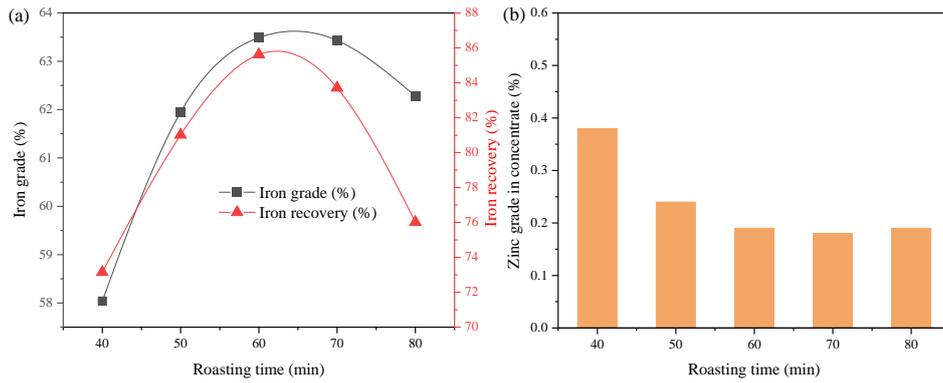
Fig. 7. Effect of roasting time: (a) iron grade and recovery, (b) zinc grade in magnetic concentrate.

Fig. 8 shows the XRD patterns of the roasting slag obtained at the different roasting times. When the roasting time was 40 min, the diffraction peak of ZnO was not observed in the XRD pattern of the roasting slag, indicating that $ZnFe_2O_4$ was not completely reduced. And, a small amount of Fe_2O_3 diffraction peaks were also observed. When the roasting time was extended to 50 min, the diffraction peak of ZnO appeared in the roasting slag, but there was still a weak diffraction peak of Fe_2O_3. The roasting time was 60 min, and there was almost no diffraction peak of Fe_2O_3 in the roasting slag. After 60 min, the diffraction peak of FeO began to appear in the roasting slag, and with the extension of roasting time, the diffraction peak of FeO gradually increased, resulting in the magnetic separation effect becoming worse.
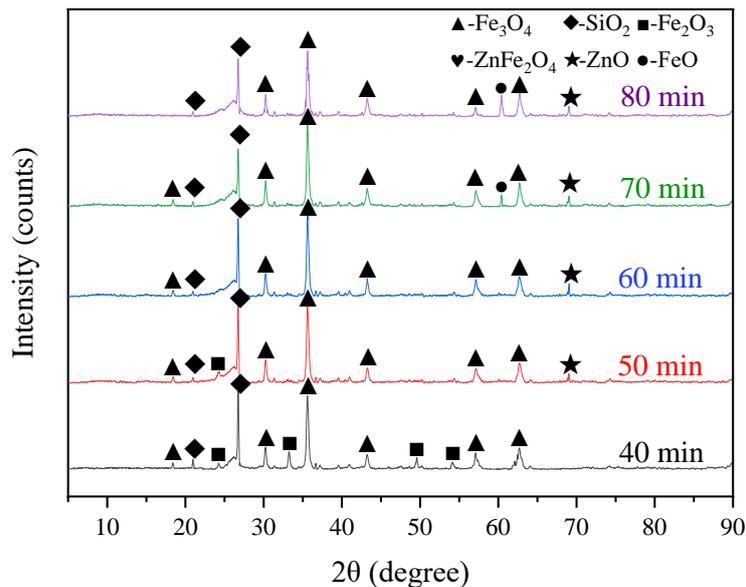
Fig. 8. XRD patterns of roasted slag with different roasting time

3.4. Thermodynamic analysis and mechanism of magnetization roasting

In this study, the purpose of magnetization roasting was to reduce hematite (Fe_2O_3) in the blast furnace dust to magnetite (Fe_3O_4) and zinc ferrite ($ZnFe_2O_4$) to magnetite (Fe_3O_4) and zinc oxide (ZnO). The reactions that occurred in the magnetization roasting process of blast furnace dust by the straw charcoal are listed as following Eqs. (2)-(15):

$$3Fe_2O_3(s) + C(s) = 2Fe_3O_4(s) + CO(g) \tag{2}$$

$$6Fe_2O_3(s) + C(s) = 4Fe_3O_4(s) + CO_2(g) \tag{3}$$

$$3Fe_2O_3(s) + CO(g) = 2Fe_3O_4(s) + CO_2(g) \tag{4}$$

$$2Fe_3O_4(s) + C(s) = 6FeO(s) + CO_2(g) \tag{5}$$

$$Fe_3O_4(s) + CO(g) = 3FeO(s) + CO_2(g) \tag{6}$$

$$2FeO(s) + C(s) = 2Fe(s) + CO_2(g) \tag{7}$$

$$FeO(s) + CO(g) = Fe(s) + CO_2(g) \tag{8}$$

$$3ZnFe_2O_4(s) + C(s) = 3ZnO(s) + 2Fe_3O_4(s) + CO(g) \tag{9}$$

$$6ZnFe_2O_4(s) + C(s) = 6ZnO(s) + 4Fe_3O_4(s) + CO_2(g) \tag{10}$$

$$3ZnFe_2O_4(s) + CO(g) = 3ZnO(s) + 2Fe_3O_4(s) + CO_2(g) \tag{11}$$

$$2ZnO(s) + C(s) = 2Zn(s) + CO_2(g) \tag{12}$$

$$ZnO(s) + C(s) = Zn(s) + CO(g) \tag{13}$$

$$ZnO(s) + CO(g) = Zn(s) + CO_2(g) \tag{14}$$

$$CO_2(g) + C(s) = 2CO(g) \tag{15}$$
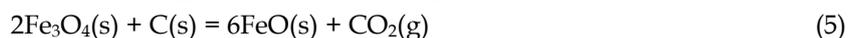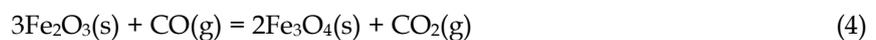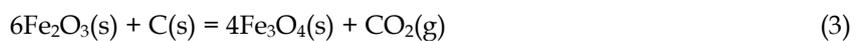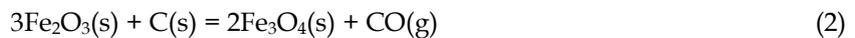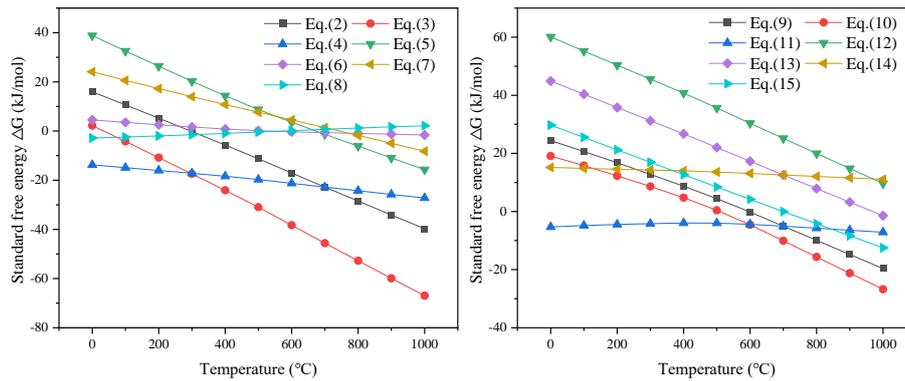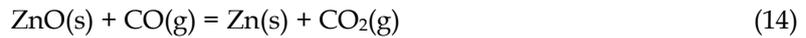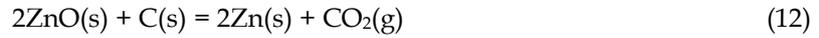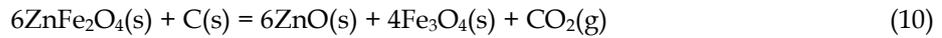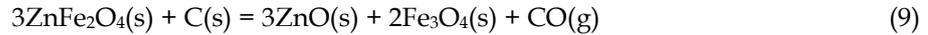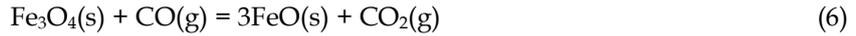
Fig. 9. Relationships between ΔG-T for main reactions of magnetization roasting process

Fig. 9 shows the standard free energy changes of the above reactions in the temperature range of 0 ℃ -1000 ℃. In the process of magnetization roasting, hematite (Fe_2O_3) in the blast furnace dust was reduced to magnetite (Fe_3O_4) phase with strong magnetism mainly through Eqs. (2)-(4). The reaction of Eq. (2) could only occur above 300 ℃, while that of Eq. (3) could occur above 200 ℃. It can be noted that the standard free energy of the reaction of Eq. (4) is negative in the whole temperature range, but when the temperature is higher than 300 ℃, the reaction of Eq. (3) is dominant. The reduction of $ZnFe_2O_4$ by carbon includes direct (Eq. (9) and (10)) and indirect (Eq. (11)) ways, and the $ZnFe_2O_4$ will be reduced to ZnO and Fe_3O_4 directly by carbon above 600 ℃ (Eq. (9) and (10)). However, when the temperature is lower than 600 ℃, $ZnFe_2O_4$ is indirectly reduced to ZnO and Fe_3O_4 by CO. When the temperature is higher than 600 ℃, the standard free energy of the direct reduction method (Eq. (10)) is lower than that of the indirect reduction method (Eq. (11)), indicating that the direct reduction method (Eq. (10)) is the main reduction method of $ZnFe_2O_4$. One of the most important points in magnetization roasting is to prevent Fe_3O_4 from being reduced to FeO, thus affecting the magnetic separation effect. It can be observed from Fig. 3 that when the temperature is higher than 700 ℃, the standard free energy of Eq. (5) and (6) is negative, indicating that Fe_3O_4 can be reduced to FeO by carbon or carbon monoxide. When the temperature is higher than 800 ℃, FeO is reduced by carbon to metallic iron, while carbon monoxide is hardly reduced FeO to metallic iron in the whole temperature range. Neither carbon nor carbon monoxide reduces ZnO to metallic zinc at 0-1000 ℃. Moreover, it can be observed that when the temperature is higher than 700 ℃, carbon dioxide and carbon can react to generate carbon monoxide by the way of Eq. (15). Based on the above analysis, hematite (Fe_2O_3) and zinc ferrite ($ZnFe_2O_4$) in the blast furnace dust are reduced to magnetite (Fe_3O_4) and zinc oxide (ZnO) with straw charcoal as the reducing agent by controlling the temperature of magnetization roasting, and then iron is recovered and zinc is enriched by magnetic separation.

To further understand the magnetization roasting process of blast furnace dust with straw charcoal as the reductant, thermogravimetric analysis was carried out on the mixed samples with the amount of straw charcoal accounting for 6% of the mass of blast furnace dust, and the results are shown in Fig. 10.

Fig. 10. TG and DTG curves of the mixed samples of blast furnace dust and straw charcoal in the N_2.

It can be seen from Fig. 10 that when the temperature increased from 25 ℃ to 100 ℃, the TG curve of the mixed samples showed an obvious downward trend. In this temperature range, the volatilization of the free water of the blast furnace dust and straw charcoal mainly occurred. When the temperature reached 100 ℃, the weight loss ratio of the mixed samples was only 1.12%. When the temperature was between 100 ℃ and 250 ℃, the TG curve decreased slowly, and the weight loss ratio of the samples was only 0.51%, indicating that no reduction reaction occurred between the blast furnace dust and the straw charcoal. The decrease in the TG curve was caused by the loss of bound water in the mixed samples. After 250 ℃, the TG curve continued to decline slowly. According to the thermodynamic analysis above, after 300 ℃, Fe_2O_3 in blast furnace dust began to reduce with carbon. However, it can be seen from Fig. 10 that when the temperature was between 250 ℃ and 450 ℃, the TG curve decreased slowly, which shows that the reduction reaction in this temperature range had not happened violently. After the temperature increased to 450 ℃, the TG curve dropped rapidly. Between 450 ℃ and 750 ℃, an obvious valley was observed in the DTG curve, which was caused by the drastic reduction reaction at this temperature. After 750 ℃, the TG curve decreased slowly, indicating that the reduction reaction was completed, and the decrease in the TG curve was caused by the further reduction of Fe_3O_4 to FeO. The thermogravimetric analysis of mixed samples was consistent with the results of the thermodynamic analysis, which explained the process and mechanism of magnetization roasting.

Fig. 11. Mechanism of recycling blast furnace dust by magnetization roasting with straw charcoal as reductant

Based on the above analysis, the mechanism diagram of recycling blast furnace dust by the magnetization roasting with the straw charcoal as the reductant is drawn, as shown in Fig. 11. When the amount of straw charcoal was 6%, the roasting temperature was 750 ℃, and the roasting time was 60 min, the reduction reaction of high furnace dust with reductant (fixed carbon and straw charcoal) occurred. Hematite (Fe_2O_3) in the blast furnace dust was reduced to Fe_3O_4 and zinc ferrite ($ZnFe_2O_4$) to Fe_3O_4 and ZnO by direct (C) and indirect (CO) reduction methods. Iron was recovered from roasting slag by low-intensity magnetic separation, while zinc was enriched in magnetic separation tailings in the form of ZnO, which could be recovered by the acid leaching.

4. Open circuit test for iron and zinc recovery

According to the optimal conditions determined in Section 3, the blast furnace dust was magnetization roasting under the conditions of 6% straw charcoal amount, 750 ℃ roasting temperature, and 60 min roasting time, and then the roasted slag was treated by the magnetic separation process. The magnetic separation experiment was performed to recover iron at the magnetic intensity of 120 kA/m. Subsequently, the magnetic separation tailings were dried and used as raw materials for zinc extraction experiments. The tailings were leached for 90 min with 0.5 mol/dm³ H_2SO_4 solution at 40 ℃ and the liquid-solid ratio of 5:1 for zinc extraction. The whole flowsheet is shown in Fig. 12.
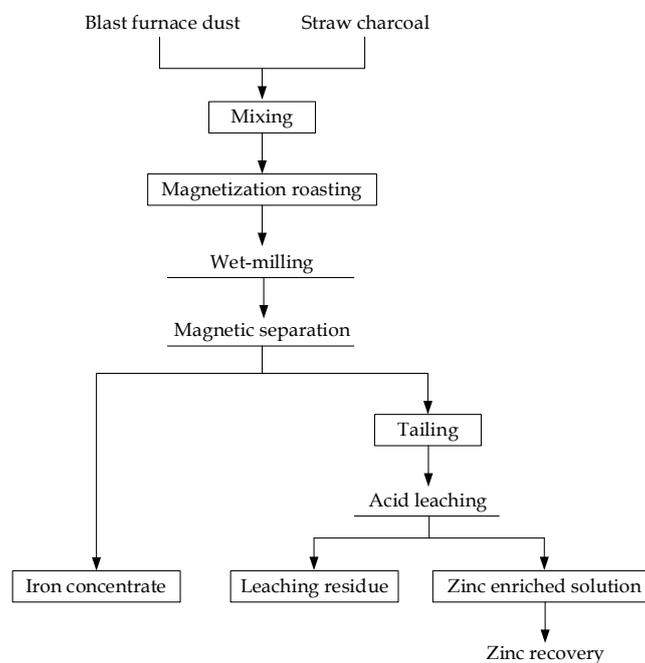
Fig. 12. The flowsheet for simultaneously recovering iron and zinc from the blast furnace dust

Under the above conditions, the roasting slag was subjected to one-stage magnetic separation, and the iron grade in magnetic concentrate was 63.50%, the iron recovery was 85.61%, and the grade of zinc in magnetic concentrate was only 0.19%. Fig. 13 showed the phase composition of roasting slag, iron concentrate, and tailings. It can be seen from Fig. 13 that the main composition phases of roasting slag were Fe_3O_4, SiO_2, and ZnO. Only a small amount of Fe_2O_3 diffraction peak with low intensity exists, indicating that Fe_2O_3 and $ZnFe_2O_4$ in the blast furnace dust were reduced to Fe_3O_4 and ZnO. The XRD pattern of magnetic concentrate showed that the main diffraction peak was Fe_3O_4, while the diffraction peak of ZnO was observed in the XRD pattern of tailings, demonstrating that iron and zinc were separated by magnetic separation after the magnetization roasting of blast furnace dust. After the leaching for the tailings with 0.5 mol/dm³ H_2SO_4 solution, it was determined that about 8.74% iron and 7.23% zinc remained in the leaching residues, indicating that 92.57% of zinc was extracted into the solution while only 5.65% of iron was co-extracted into the zinc-rich solution. Table 4 shows the chemical composition of iron concentrate, it can be seen from Table 4 that iron concentrate contains a

small number of impurities such as silicon, calcium, and sulfur, so it can be used as an ingredient in iron-making.

At present, the research on the recovery of the blast furnace dust mainly focuses on the separation of zinc and iron by high-temperature calcination, the calcination temperature is usually above 1000 ℃ (Lin et al., 2017). For example, Hu et al. (Hu et al., 2018) found that high-grade zinc smelting materials could be collected from the flue gas when the blast furnace dust was heated to 1150 ℃. Some researchers have studied the selective extraction of zinc from the blast furnace dust by the hydrometallurgical process. For example, Halli et al. (Halli et al., 2017) studied the selective leaching of zinc from the electric arc furnace dust by the direct leaching method and found that the leaching efficiency of zinc was more than 75% and that of iron was less than 6% by leaching with 10% aqua regia or 1.2 mol/dm³ hydrochloric acid. In this study, the process proposed of recycling blast furnace dust by the magnetization roasting magnetic can decompose zinc ferrite in the blast furnace dust by magnetic roasting at a lower temperature (750 ℃), and then recover iron and zinc by magnetic separation and leaching respectively. The proposed flowsheet for simultaneously recovering iron and zinc from the blast furnace dust may provide a new idea for the treatment and utilization of blast furnace dust.
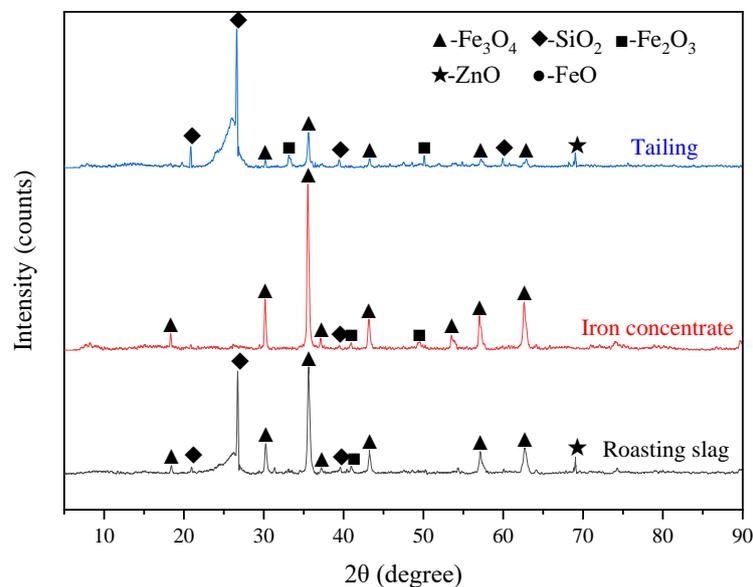
Fig. 13. XRD patterns of roasting slag, iron concentrate, and tailing

Table 4. Main chemical components of iron concentrate

Elements	Fe	Si	Ca	S	Zn	Al	Mn
Contents (%)	63.50	1.14	0.63	0.43	0.19	0.14	0.11

5. Conclusions

In this study, the process of recycling blast furnace dust by the magnetization roasting with the straw charcoal as a reductant is the proposed. Under the conditions of straw charcoal amount of 6%, the roasting temperature of 750 ℃, and the roasting time of 60 min, hematite (Fe_2O_3) and zinc ferrite ($ZnFe_2O_4$) in the blast furnace dust were reduced to Fe_3O_4 and ZnO. Then, iron concentrate with an iron recovery of 85.61% and iron grade of 63.50% was obtained by magnetic separation at the magnetic intensity of 120 kA/m. Meanwhile, the grade of zinc in magnetic concentrate was 0.19%, indicating that most of the zinc was enriched in the tailings. Zinc would be recovered from magnetic tailings containing ZnO by the existing zinc hydrometallurgy process. In addition, the proposed process for simultaneously recovering iron and zinc from the blast furnace dust could achieve that 85.61% of iron was recovered, 92.57% of zinc was extracted into solution, while only 5.65% of iron was co-extracted into zinc-rich solution. The straw charcoal in this study was innovatively used as the reductant to replace traditional anthracite, which not only saved non-renewable fossil fuels but also

reduced harmful gas emissions in the magnetization roasting process due to the sulfur content of straw charcoal is much lower than that of anthracite.

Acknowledgments

References

ASADI ZEYDABADI, B., MOWLA, D., SHARIAT, M.H., FATHI KALAJAHI, J., 1997. *Zinc recovery from blast furnace flue dust.* Hydrometallurgy. 47(1), 113-125.

CHUN, T.J., ZHU, D.Q., 2015. *New Process of Pellets-Metallized Sintering Process (PMSP) to Treat Zinc-Bearing Dust from Iron and Steel Company.* Metall Mater Trans B. 46(1), 1-4.

DAS, B., PRAKASH, S., REDDY, P.S.R., MISRA, V.N., 2007. *An overview of utilization of slag and sludge from steel industries.* Resour Conserv Recy. 50(1), 40-57.

GUO, X.S., LI, Z.Y., HAN, J.C., YANG, D., SUN, T.C., 2021. *Study of Straw Charcoal as Reductant in Co-reduction Roasting of Laterite Ore and Red Mud to Prepare Powdered Ferronickel.* Mining Metall Explor. 38(5), 2217-2228.

HAJINAJAF, N., MEHRABADI, A., TAVAKOLI, O., 2021. *Practical strategies to improve harvestable biomass energy yield in microalgal culture: A review.* Biomass Bioenerg. 145, 105941.

HALLI, P., HAMUYUNI, J., REVITZER, H., LUNDSTRÖM, M., 2017. *Selection of leaching media for metal dissolution from electric arc furnace dust.* J Clean Prod. 164, 265-276.

HU, T., LV, X.W., BAI, C.G., 2016. *Enhanced Reduction of Coal-Containing Titanomagnetite Concentrates Briquette with Multiple Layers in Rotary Hearth Furnace.* Steel Res Int. 87(4), 494-500.

HU, W.T., WANG, H.J., LIU, X.W., SUN, C.Y., 2014. *Effect of nonmetallic additives on iron grain grindability.* Int J Miner Process. 130, 108-113.

HU, W.T., LIU, X.W., WANG, H.J., DAI, X.J., PAN, D.L., LI, J., SUN, C.Y., XIA, H.W., WANG, B., 2017. *Improvement of Sodium Leaching Ratio of Ferric Bauxite Sinter after Direct Reduction.* Minerals-Basel. 7(1).

HU, W.T., XIA, H.W., PAN, D.L., WEI, X.L., LI, J., DAI, X.J., YANG, F., LU, X., WANG, H.J., 2018. *Difference of zinc volatility in diverse carrier minerals: The critical limit of blast furnace dust recycle.* Miner Eng. 116, 24-31.

KANABKAEW, T., NGUYEN, T.K.O., 2011. *Development of Spatial and Temporal Emission Inventory for Crop Residue Field Burning.* Environ Model Assess. 16(5), 453-464.

LANZERSTORFER, C., BAMBERGER-STRASSMAYR, B., PILZ, K., 2015. *Recycling of Blast Furnace Dust in the Iron Ore Sintering Process: Investigation of Coke Breeze Substitution and the Influence on Off-gas Emissions.* ISIJ Int. 55(4), 758-764.

LANZERSTORFER, C., 2017. *Characterization of dust from blast furnace cast house de-dusting.* Environ Technol. 38(19), 2440-2446.

LECLERC, N., MEUX, E., LECUIRE, J.M., 2002. *Hydrometallurgical recovery of zinc and lead from electric arc furnace dust using mononitrilotriacetate anion and hexahydrated ferric chloride.* J Hazard Mater. 91(1), 257-270.

LI, Y.C., LIU, H., PENG, B., MIN, X.B., HU, M., PENG, N., YUANG, Y.Z., LEI, J., 2015. *Study on separating of zinc and iron from zinc leaching residues by roasting with ammonium sulphate.* Hydrometallurgy. 158, 42-48.

LIN, X., PENG, Z., YAN, J., LI, Z., HWANG, J.Y., ZHANG, Y., LI, G., JIANG, T., 2017. *Pyrometallurgical recycling of electric arc furnace dust.* J Clean Prod. 149, 1079-1100.

LIU, C., SUN, Y., LI, N., ZHANG, B., LIU, J., 2019. *Improved energy utilization efficiency via adding solar radiant heating mode for traditional bioreactor to dispose straw: Experimental and numerical evaluation.* Waste Manage. 89, 303-312.

LUO, X., WANG, C., SHI, X., LI, X., WEI, C., LI, M., DENG, Z., 2022. *Selective separation of zinc and iron/carbon from blast furnace dust via a hydrometallurgical cooperative leaching method.* Waste Manage. 139, 116-123.

MAKKONEN, H.T., HEINO, J., LAITILA, L., HILTUNEN, A., PÖYLIÖ, E., HÄRKKI, J., 2002. *Optimisation of steel plant recycling in Finland: dusts, scales and sludge.* Resour Conserv Recy. 35(1), 77-84.

MANSFELDT, T., DOHRMANN, R., 2004. *Chemical and mineralogical characterization of blast-furnace sludge from an abandoned landfill.* Environ Sci Technol. 38(22), 5977-5984.

NAYAK, N.P., 2022. *Characterization of blast furnace flue dust- an assessment for its utilization.* Mater Today. 50, 2078-2083.

SEGLAH, P.A., WANG, Y., WANG, H., BI, Y., ZHOU, K., WANG, Y., WANG, H., FENG, X., 2020. *Crop straw utilization and field burning in Northern region of Ghana*. J Clean Prod. 261, 121191.

SHEN, L., QIAO, Y., GUO, Y., TAN, J., 2010. *Preparation of nanometer-sized black iron oxide pigment by recycling of blast furnace flue dust.* J Hazard Mater. 177(1), 495-500.

STEER, J.M., GRIFFITHS, A.J., 2013. *Investigation of carboxylic acids and non-aqueous solvents for the selective leaching of zinc from blast furnace dust slurry.* Hydrometallurgy 140, 34-41.

WU, S.L., CHANG, F., ZHANG, J.L., LU, H., 2017. *Kinetics and Reduction Behavior of Self-reducing Briquettes Containing Blast Furnace Dust, 8th International Symposium on High-Temperature Metallurgical Processing*. San Diego, CA, pp. 591-601.

WU, Y.L., JIANG, Z.Y., ZHANG, X.X., XUE, Q.G., MIAO, Z., ZHOU, Z., SHEN, Y.S., 2018. *Process optimization of metallurgical dust recycling by direct reduction in rotary hearth furnace*. Powder Technol. 326, 101-113.

XU, J., WANG, N., CHEN, M., ZHOU, Z., YU, H., 2020. *Comparative investigation on the reduction behavior of blast furnace dust particles during in-flight process in hydrogen-rich and carbon monoxide atmospheres.* Powder Technol. 366, 709-721.

YANG, X., CHU, M., SHEN, F., ZHANG, Z., 2009. *Mechanism of zinc damaging to blast furnace tuyere refractory.* Acta Metall Sin-Engl. 22(6), 454-460.

YE, L., PENG, Z., YE, Q., WANG, L., AUGUSTINE, R., PEREZ, M., LIU, Y., LIU, M., TANG, H., RAO, M., LI, G., JIANG, T., 2021. *Toward environmentally friendly direct reduced iron production: A novel route of comprehensive utilization of blast furnace dust and electric arc furnace dust.* Waste Manage. 135, 389-396.

ZHANG, D., ZHANG, X., YANG, T., RAO, S., HU, W., LIU, W., CHEN, L., 2017. *Selective leaching of zinc from blast furnace dust with mono-ligand and mixed-ligand complex leaching systems.* Hydrometallurgy 169, 219-228.

ZHANG, D., LING, H., YANG, T., LIU, W., CHEN, L., 2019. *Selective leaching of zinc from electric arc furnace dust by a hydrothermal reduction method in a sodium hydroxide system*. J Clean Prod. 224, 536-544.

ZHONG, R., YI, L., HUANG, Z., SHEN, X., JIANG, T., 2018. *Sticking mechanism of low grade iron ore-coal composite in rotary kiln reduction.* Powder Technol. 339, 625-632.